Chapter – 4

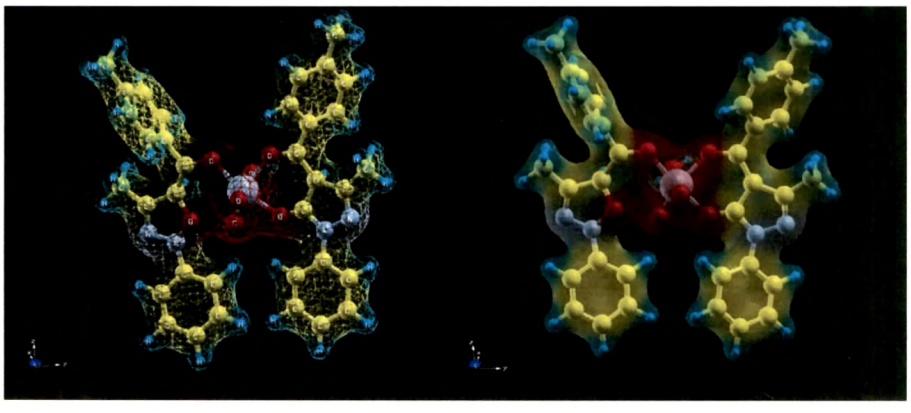

Computational studies on oxovanadium(IV) complexes of acylpyrazolone ligands using DFT method

4.1 Introduction

Theoretical chemistry is the subfield where mathematical methods are combined with fundamental laws of physics to study processes of chemical relevance [1]. Computational chemistry is an exciting and fast-emerging discipline which deals with the modeling and the computer simulation of systems such as biomolecules, polymers, drugs, inorganic and organic molecules, and so on. Computational chemistry has grown to the state it is today and it became popular being immensely benefited from the tremendous improvements in computer hardware and software during the last several decades. With high computing power using parallel or grid computing facilities and with faster and efficient numerical algorithms, computational chemistry can be very effectively used to solve complex chemical and biological problems [2].

Computational chemistry is comprised of a theoretical (or structural) modeling part, known as molecular modeling, and a modeling of processes (or experimentations) known as molecular simulation. Depending upon the level of theory that we observe in a computation, the following five broad classes have been described below.

1. **Molecular Mechanics (MM):** Molecular mechanics is based on a model of a molecule as a collection of balls (atoms) held together by springs (bonds). If we know the normal spring lengths and the angles between them, and how much energy it takes to stretch and bend the springs, we can calculate the energy of a given collection of balls and springs, i.e. of a given molecule; changing the geometry until the lowest energy is found enables us to do a geometry optimization, i.e. to calculate a geometry for the molecule. Molecular mechanics is fast and can optimize a large molecule like cholesterol in seconds on a powerful desktop computer (a workstation).
2. **Ab Initio Calculations:** The term *Ab initio* is the Latin term meaning "from the beginning." This name is specified to computations which are derived directly from the theoretical principles such as Schrödinger equation, with no inclusion of experimental data. Schrödinger equation is one of the fundamental equations of modern physics and describes how the electrons behave in a molecule. The *Ab initio* method solves the Schrödinger equation

for a molecule and gives us the molecule's energy and wavefunction. The wavefunction is a mathematical function that can be used to calculate the electron distribution.

The most common type of *Ab initio* calculation is called a Hartree Fock calculation (HF), in which the primary approximation is called the central field approximation. This method does not include Coulombic electron-electron repulsion in the calculation. However, its net effect is included in the calculation.

3. **Semiempirical (SE) calculations:** semiempirical calculations are similar to ab initio, based on the Schrödinger equation. However, more approximations are made in solving it, certain pieces of information, such as two electron integrals, are approximated or completely omitted. Consecutively to correct the error introduced by omitting part of the calculation, the method is parameterized, by curve fitting in a few parameters or numbers, in order to give the best possible agreement with experimental data. Semiempirical calculations are slower than MM but much faster than ab initio calculations. Semiempirical calculations have been very successful in the description of organic chemistry, where there are only a few elements used extensively and the molecules are of moderate size. However, semiempirical methods have been devised specifically for the description of inorganic chemistry as well.
4. **Density functional calculations or Density functional method (DFT):** DFT calculations are similar to ab initio and semi empirical calculations, however, unlike the other two methods DFT does not calculate a wavefunction, but rather derives the electron distribution (electron density function) directly. A function is a mathematical entity related to a function. DFT methods based on approximate solutions of the Schrödinger equation, bypassing the wavefunction that is a central feature of ab initio and semiempirical medhods. Density functional calculations are usually faster than ab initio, but slower than SE.
5. **Molecular dynamics calculations:** Molecular dynamics calculations study the molecules in motion and apply the laws of motion to molecules. Thus one can simulate the motion of an enzyme as it changes shape on binding to a substrate, or the motion of a swarm of water molecules around a molecule of solute.

Currently density functional theory (DFT) is commonly used to examine the electronic structure of transition metal complexes. It meets with the requirements of being accurate, easy to use and fast enough to allow the study of relatively large molecules of transition metal complexes.

The past years have seen development of powerful methods based on density functional theory (DFT) and on resolution of identity approximations; together with significant progress on computer capacity the application of high-level quantum calculations to realistic chemical and/or biological systems still exceeds the present capacity of most research groups [3]. Many studies have been published testing the performance of density functional theory (DFT) in the determination of the structures and energetics of transition metal compounds [4].

In recent years, density functional theory (DFT) has been extensively used in theoretical modeling. The development of better exchange–correlation functionals has made it possible to calculate many molecular properties with comparable accuracies to traditionally correlated *ab initio* methods, with more favorable computational costs [5]. A literature survey revealed that the DFT has a great accuracy in reproducing the experimental values in geometry, dipole moment, vibrational frequency, etc [6]. (E)-2-[(2-Chlorophenyl)iminomethyl]-4-trifluoromethoxyphenol was synthesized and characterized by single crystal XRD and other spectroscopic techniques [6*a*]. The crystal structure results show that show that the compound exists in the enol-imine form, which is stabilized by the intramolecular O-H···N hydrogen bond. The electronic structure of the compound calculated by DFT method was compared with the experimental data, leading to a very closer agreement with the experimental results.

A series of copper halides with selone and thione ligands was synthesized and their crystal structures were determined by Brumaghim *et al,* DFT calculations on the synthesized copper complexes was performed and the theoretical bond lengths and bond angles were compared with the experimental crystal structure data [7]. DFT calculations show good correlation to the observed X-ray structures for the complexes. Baitalik *et al*, presented a combined experimental and DFT investigation on the structural and electronic properties of mixed-ligand monometallic osmium(II) complexes [8].

A series of Hg(II)–NH carbene complexes of annulated ligand pyridinyl[1,2-a]{2-pyridylimidazol}-3-ylidene hexaflurophosphate was synthesized and their geometries were determined by the single crystal XRD [9]. DFT calculations provide geometrical parameters in conformity with the experimental values. The molecules prefer *syn* configuration over the *anti* due to lower energy supported by theoretical studies. Copper complexes of pyridine-2,6-dicarboxylate and N-donor neutral ligands were synthesized and their molecular structure was obtained by single crystal X-ray analysis [10]. The electronic and IR spectra of these compounds are compared with results obtained by employing DFT and time-dependent density functional theory (TD-DFT) calculations. The optimized geometry from density functional theory (DFT) study shows a good agreement with the X-ray structural data.

Wolff *et al* have synthesized and characterized dioxorhenium complexes of various nitrogen containing heterocyclic ligands [11]. The X-ray crystal structures of the complexes were determined and the electronic structures were examined using the density functional theory (DFT) method. The experimental and theoretical results were compared and showed a good agreement with the X-ray structural data and appropriate prediction of the UV-Vis spectra.

Vanadium is a widely dispersed element, making up about 0.014% of the Earth's crust and it is the 5th most abundant transition metal. The interest in the chemistry of oxovanadium complexes has grown enormously over the last few decades due to the role of vanadium in several biological [12] and catalytic [13] processes. The precise knowledge of the chemical properties of new vanadium derivatives may provide valuable information with respect to the behavior of such complexes in biological and catalytic systems. Its rich coordination chemistry, especially in oxidation states +3, +4 and +5, involving mainly V-O, V-N and V-S bonds, affords many stereochemically flexible complexes. Thus, the coordination chemistry of vanadium, in the high oxidation states (IV and V), continues to be intensively explored, as shown also by some recent contributions [14]. DFT study has played an important role in studying the geometrical properties of vanadium complexes.

Pessoa *et al syn*thesized vanadium(IV/V) complexes of N,N'-ethylenebis-(pyridoxylideneiminato) and N,N'-ethylenebis(pyridoxylaminato). The geometries of

these complexes were established by single-crystal XRD and DFT calculations. The bond lengths and bond angles obtained by single-crystal XRD data and DFT calculations were compared. The calculations were performed with the B3LYP HF/DFT hybrid functional as implemented in the Gaussian 98 set of programs [15]. The crystal structure data and the results obtained from DFT calculation were compared and found to be similar. Numerous reports are available in the literatures in which experimental data were compared with the theoretical data to establish the structure of vanadium complexes. The energies of complexes were also calculated to understand the stable conformations of the complexes [16].

The coordination chemistry and reactivity of transition metal complexes containing 4-acyl pyrazolone ligands have attracted considerable research interests [17]. This versatile class of ligands reacts with simple, commercially available metal precursors to give metal complexes which provide opportunities for investigations of catalytic [18-21] as well as biological applications [22]. Due to the presence of two oxygen donor atoms and facile keto– enol tautomerism, they easily coordinate with metal ions after deprotonation of the enolic hydrogen and provide stable metal complexes with six-member chelate rings.

Recently, we have directed our investigations into the coordination chemistry of vanadium complexes of acylpyrazolone ligands and their catalytic properties [20, 21]. The literatures [23] shows that in the past many analytical and spectroscopic studies have been carried out to investigate the geometry of oxovanadium(IV) complexes of acylpyrazolone, but there was no crystal structure evidence to support the proposed structures/geometry. The first crystal structure evidence was provided by Fabio *et al* [19], having *anti* conformation of acylpyrazolone ligands around the metal ion. The *syn*thesis and crystal structure of an oxovanadium(IV) complex with an acylpyrazolone ligand has been recently reported by our group [20]. During our investigation, interestingly, we found that in oxovanadium(IV) complex of 1-Phenyl-3-methyl-4-touloyl-5-pyrazolone (complex **1**) the ligands are in *syn* configuration to each other creating distorted octahedral environment around the metal ion. Therefore, we have focused our attention in studies on the structural investigation of oxovanadium(IV) complexes with acylpyrazolone ligands. We have also *syn*thesized an oxovanadium(IV) complex of 1-touloyl-3-methyl-4-phenyl-5-pyrazolone,

developed its single crystal structure and characterized by X-ray single crystal analysis [21]. One acetonitrile molecule has also been trapped in the crystal lattice of the complex. Somewhat surprisingly, in the complex **2** the coordination mode of ligands with centre metal has been changed and the ligands are in twisted configuration to each other creating distorted octahedral environment around the vanadium ion. The difference in the geometry of the *syn*thesized complexes and other reported literatures motivated us to calculate the electronic structure of oxovanadium(IV) complexes with the use of density functional theory (DFT) method and compare the results with experimental data. DFT describes the electronic states of atoms and molecules in terms of the three-dimensional electronic density of the system. DFT calculations have been performed on both the complexes, complex **1** (*syn* conformation and *anti* conformation) and complex **2** (with solvent and without solvent).

To the best of our knowledge, the experimental molecular structures, detailed structural analysis and electronic properties of the oxovanadium(IV) complexes of acylpyrazolone complexes have not been studied yet. Therefore, this theoretical study aimed to determine the molecular structures and highest occupied molecular orbital (HOMO) and lowest unoccupied molecular orbital (LUMO) properties of oxovanadium(IV) complexes of acylpyrazolone due to their important role in the catalytic properties. In addition, their electronic properties, such as HOMO and LUMO energies and density of states have been also calculated and discussed using DFT.

In this chapter we clarify the nature of HOMO and LUMO with optimized geometries by studying its electronic properties and discuss their consequences. This understanding can be further used to model other ligands having similar or even better properties. The rest of the chapter is divided in three parts. In Section 'Experimental and computational details', we have given a detailed description of the computational methods we employed in present calculations. The obtained structural parameters, electronic densities of states and HOMO and LUMO are discussed in Section 'Results and discussion'. Finally in Section 'Conclusion' important conclusions are presented.

4.2 Experimental and Computational details

The *syn*thesis of complex **1** and complex **2** were described in the Part 1 of Chapter 1. As a first step in our calculations, the constructed model structures for complex **1** (*syn* and *anti* configuration) and complex **2** (with solvent and without solvent) were allowed to relax. This was done by using Broyden-Fletcher-Goldfarb-Shanno (BFGS) method. We use plane wave density functional (perturbation) theory implementation in PWSCF simulation package [24]. The wave function describes only the valence and conduction electrons, while the core electrons are taken into account using the pseudopotentials. The kinetic energy cutoff for the plane wave basis is set to 25 Ry and the Brillouin zone (BZ) is at gamma sampled for the relaxation of the complex **1** (*syn* and *anti* configuration) and complex **2** (with solvent and without solvent) and density of states calculation are performed by 1×1×1 Monkhorst-Pack *k*-point mesh [25]. A careful convergence has been set up for kinetic energy cut off and the number of k-points in discretized BZ represented by Monkhorst-Pack meshes. Both atomic positions and cell parameters were optimized until all the residual forces were smaller than 0.01 eV/Å. For the response function calculations we used only the highly transferable GGA potentials of PBE type for the optimization of atomic positions and unit cell parameters and electronic properties. In order to gain better insight into the electronic properties including the HOMO and LUMO of the complexes all the structures were recalculated using GAUSSIAN03 package [26]. For the calculations with GAUSSIAN03, we have used the B3LYP functional composed of Beek's three (B3) parameter hybrid exchange functional and correlation functions of Lee, Yang and Parr (LYP) [27] and all electron 6–31 G(d,p) basis set including polarization functional for atoms. The geometry and total energy were not much sensitive to the basis set but the relative energies and energy gaps between HOMO and LUMO results from the inclusion of hybrid functionals.

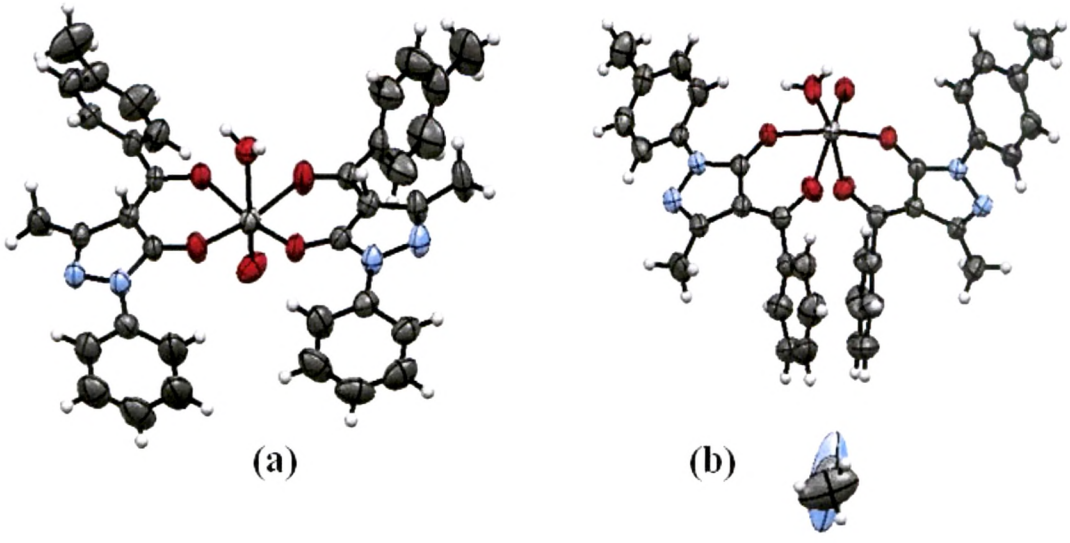

Figure 4.1. (*a*) Crystal structure of complex **1** having both the ligands in *syn* conformation, (*b*) crystal structure of complex **2** having both the ligands in *twisted* form.

4.3 Results and Discussion

The crystal structures of the complex **1** and complex **2** were obtained by us in our previous reports [13, 14]. Both the complexes belong to the space group $P2_1/c$. The lattice parameters of the complex 1 & 2 are a = 13.6618(12) , b = 27.5554(17), c = 9.7253(10)Å, V = 3540.6(5)Å^3 and a = 17.2079(7), b = 11.4667(5), c = 18.6877(8)Å, V = 3558.5(3)Å^3, respectively. The molecular structures of the complexes **1** and **2** are illustrated in the Figure 4.1.

4.3.1 Molecular geometry

The molecular structures of complex **1** in both *anti* and *syn* conformations and complex **2** with and without solvent were studied by DFT methods. The starting coordinates for the complex **1** and complex **2** were those obtained by X-ray diffraction and were optimized by energy minimization with the DFT method (*see* Figure 4.2).

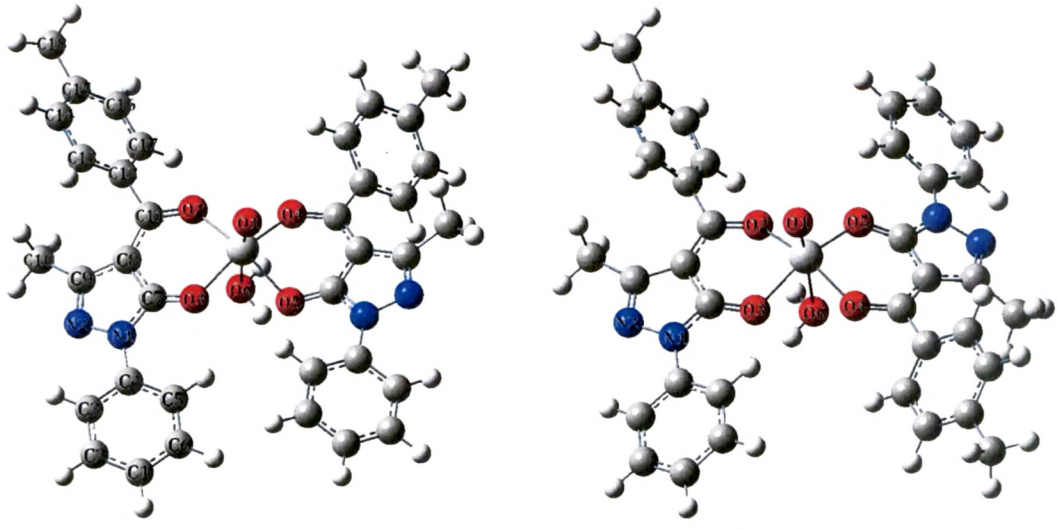

(*a*) *Syn* conformation (*b*) *Anti* conformation

Figure 4.2. Optimized structures of complex **1** (a) *syn* configuration and (b) *anti* configuration.

Table 4.1. Experimental and theoretical bond lengths of complex **1** in the *syn* and *anti* conformations.

Bond lengths	Experimental values (Å)	Optimized *syn* conformation (Å)	Optimized *anti* conformation (Å)
V1-O1	1.593	1.624	1.911
V1-O2	1.999	2.057	2.123
V1-O3	1.969	1.920	2.325
V1-O4	2.022	2.021	2.470
V1-O5	1.978	1.924	1.615
V1-O6	2.247	1.959	2.016

There is remarkably good agreement between the X-ray data for the oxovanadium(IV) complex **1** and the data for the optimized structure of the *syn* conformation. In the *syn* conformation bond lengths of all the oxygen atoms (O1-O6) with central metal (V1) are in good agreement with the crystal structure data. However, in the optimized structure of *syn* conformation bond length of the coordinated water molecule with vanadium atom (V1-O6) decreased by 0.288 Å. The comparison of the bond lengths and bond angles of crystal structure and optimized structures of complex **1** are summarized in Table 4.1.

Since the theoretical results of the optimized geometry of *syn* configuration agree closely with the experimental values, we then proceeded to the molecular structure of the *anti* configuration with the coordinates of oxovanadium(IV) complex **1** described above. The V1-O1 bond length is increased by 0.318°, while bond lengths V1-O5 (V=O) & V1-O6 (V-OH_2) are decreased by 0.361° and 0.231°, respectively. Thus, the bond lengths of *anti* configuration differ with the few % Å of experimental results.

The comparison of bond angles of experimental and theoretical results is shown in Table 4.2. The bite angles O1-V1-O2 and O3-V1-O4 in the optimized structure of *syn* configuration are comparable with the experimental results. The angle between V=O group and coordinated water molecule (O5-V1-O6) decreases a little by 7.98°. The angle O2-V1-O4 increases by 13.35°.

Table 4.2. Experimental and theoretical bond angles of the *syn* and *anti* conformations.

Bond angles (°)	Experimental values (°)	Optimized *syn* conformation (°)	Optimized *anti* conformation (°)
O1-V1-O2	90.24(13)	93.948	50.860
O3-V1-O4	88.31(13)	79.166	55.044
O5-V1-O6	175.42(19)	167.437	137.33
O1-V1-O4	162.72(14)	160.25	129.01
O1-V1-O6	83.03(15)	79.79	62.90
O2-V1-O6	81.18(15)	76.16	105.77
O2-V1-O4	89.58(13)	102.93	158.18
O1-V1-O3	87.49(13)	84.58	155.27
O2-V1-O3	165.30(15)	176.23	136.71
O3-V1-O6	84.13(15)	106.93	94.48
O4-V1-O6	79.87(14)	94.23	89.12
O1-V1-O5	100.31(16)	109.63	117.96
O2-V1-O5	95.60(18)	94.51	68.11
O3-V1-O5	99.10(18)	82.75	71.06
O4-V1-O5	96.91(16)	111.45	70.794

The dihedral angle between the plane P_1 (C23O1V1O2C33C24) and P_2 (C3O3V1O13C13C4) of the optimized structure of *syn* configuration is 17.21°, while the experimentally determined dihedral angle is 9.75° (*see* Figure 4.3).

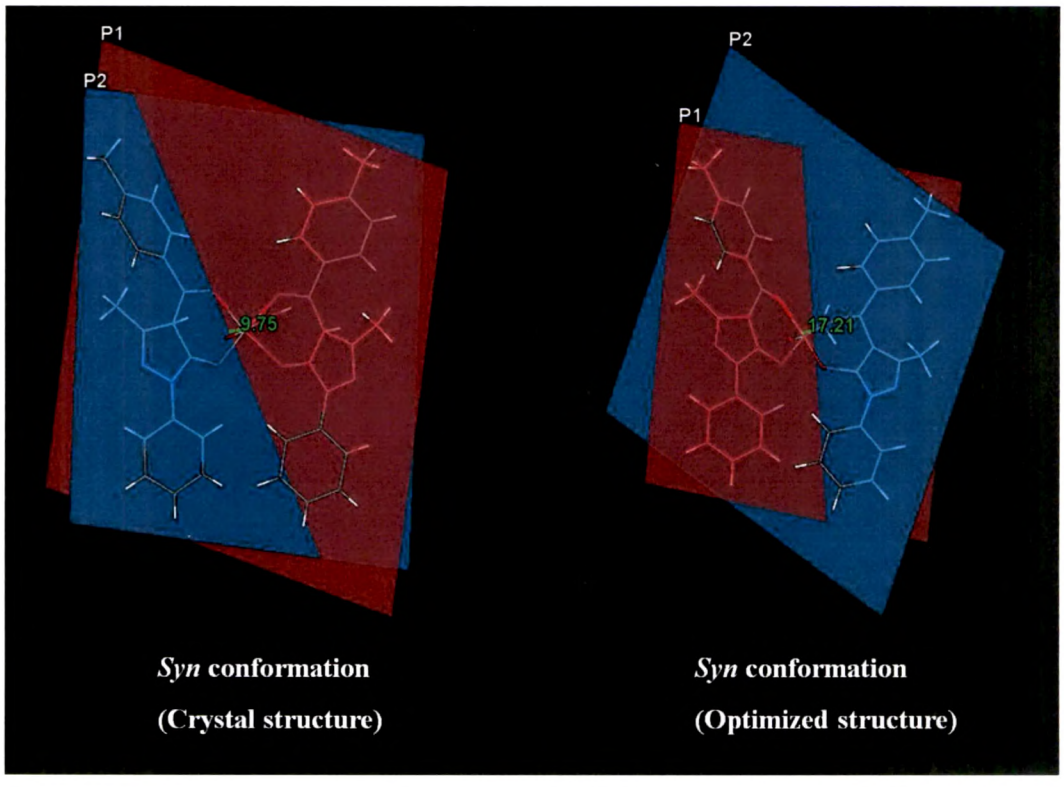

Figure 4.3. Dihedral angle between the plane P_1 (C23O1V1O2C33C24) and P_2 (C3O3V1O13C13C4) of the (*a*) crystal structure and (*b*) optimized structure in *syn* conformation.

All other angles are in good agreement with the optimized *syn* configuration of complex **1**. The bite angles O1-V1-O2 and O3-V1-O4 in the optimized structure of *anti* configuration decrease by 39.38° and 33.27°, respectively. The angles O1-V1-O3 and O2-V1-O4 are increased by 67.78° and 68.6°, respectively. Other anglers in the optimized *anti* configuration of complex **1** also have deviated from the experimental results. The comparison of bond lengths and bond angles results show that in the complex **1** *syn* conformation is dominant over the *anti* configuration. The total energies of *syn* as well as *anti* conformation were also calculated. The calculated total energy for *syn* conformation is -10.162 keV, while total energy for *anti* conformation is -10.155 keV. The total energy of *syn* conformation is less than the *anti* conformation. Thus, *syn* conformation is more stable than the *anti* conformation.

The optimization of geometry has also been carried out for the complex **2**, with solvent and without solvent. The geometries of the optimized structures of the complex **2**, with solvent and without solvent are illustrated in the Figure 4.4.

There is a good agreement between the X-ray data for the oxovanadium(IV) complex **2** and data for the optimized structure for the complex with solvent. In the optimized structure with solvent bond lengths of all the oxygen atoms (O1-O6) with V1 are in good agreement with the crystal structure data. In the optimized structure of complex **2** with solvent the bond length V1-O6 increases by 0.1826 Å, while the bond lengths V1-O2 and V1-O3 decrease little by 0.039 and 0.051 Å, respectively. The comparison between calculated and experimental values of bond lengths is presented in Table 4.3.

Table 4.3. Experimental and theoretical bond lengths of the complex **2** (with solvent and without solvent).

Bond lengths	Experimental value (Å)	Optimized structure With solvent (Å)	Optimized structure Without solvent (Å)
V1-O1	1.982	2.01068	1.60819
V1-O2	2.021	1.98194	2.02699
V1-O3	2.018	1.96735	2.02963
V1-O4	2.205	2.19723	2.06512
V1-O5	1.594	1.60263	1.89988
V1-O6	2.022	2.20456	2.13641

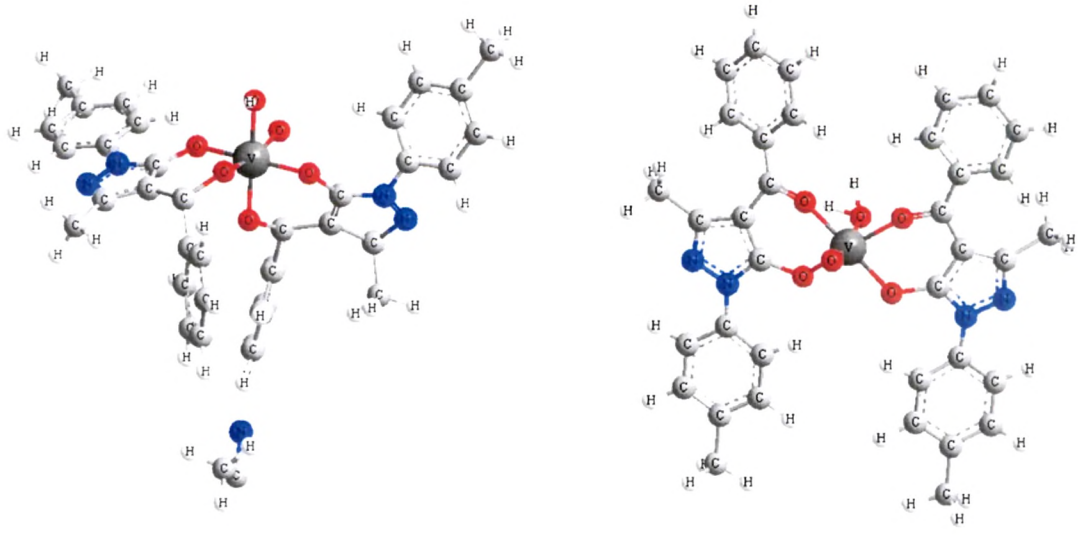

(*a*) **Complex 2 with solvent** (*b*) **Complex 2 without solvent**

Figure 4.4. Optimized structures of complex **2** (*a*) with solvent and (*b*) without solvent.

The theoretical results of the optimized geometry of complex **2** with solvent agree well with the experimental data, we further moved to the optimization of molecular structure of the complex **2** without solvent with the coordinates of oxovanadium(IV) complex **2** described above. The bond lengths V1-O1 and V1-O4 were found to decrease by 0.374 and 0.134 Å, respectively, while the bond lengths V1-O5 (V=O) and V1-O6 (V-OH_2) were found to increase by 0.306 and 0.114, respectively. The comparison of bond lengths results that the structure without solvent differs from the experimentally obtained structure.

The comparison of bond angles of experimental and theoretical results is presented in Table 4.4. The bite angles O1-V1-O2 and O3-V1-O4 in the case of optimized structure with solvent are in good agreement with the experimental data. There is a small variation of 7.02° between the coordinated water molecule and oxo group (O5-V1-O6). All other bond angles of the optimized structure with solvent are in good agreement with the experimental values.

Table 4.4. Experimental and theoretical bond angles of the complex **2** (with solvent and without solvent) with the experimental values.

Bond angles	Experimental values (°)	Optimized structure with solvent (°)	Optimized structure without solvent (°)
O1-V1-O2	91.06 (9)	90.93	53.38
O3-V1-O4	83.19 (8)	83.06	57.60
O5-V1-O6	98.8 (1)	91.78	179.28
O1-V1-O4	82.22 (8)	81.96	163.49
O1-V1-O6	86.8 (1)	86.70	64.38
O2-V1-O6	162.1 (1)	165.66	117.46
O2-V1-O4	79.13 (9)	83.42	125.14
O1-V1-O3	165.23 (9)	164.30	126.50
O2-V1-O3	88.48 (9)	91.99	172.30
O3-V1-O6	89.1 (1)	86.66	62.18
O4-V1-O6	83.0 (1)	82.24	116.08
O1-V1-O5	99.1 (1)	97.12	115.02
O2-V1-O5	99.0 (1)	102.55	61.98
O3-V1-O5	95.5 (1)	97.29	118.44
O4-V1-O5	177.8 (1)	173.99	64.38

The dihedral angle between the plane P_1(C23O1V1O2C33C24) and P_2(C3O3V1O13C13C4) of the optimized structure with solvent is 75.36° indicates an overall good agreement, while the experimentally determined dihedral angle is 73.21° (*see* Figure 4.5). The bite angles O1-V1-O2 and O3-V1-O4 in the optimized structure without solvent decrease by 37.68° and 25.59°, respectively.

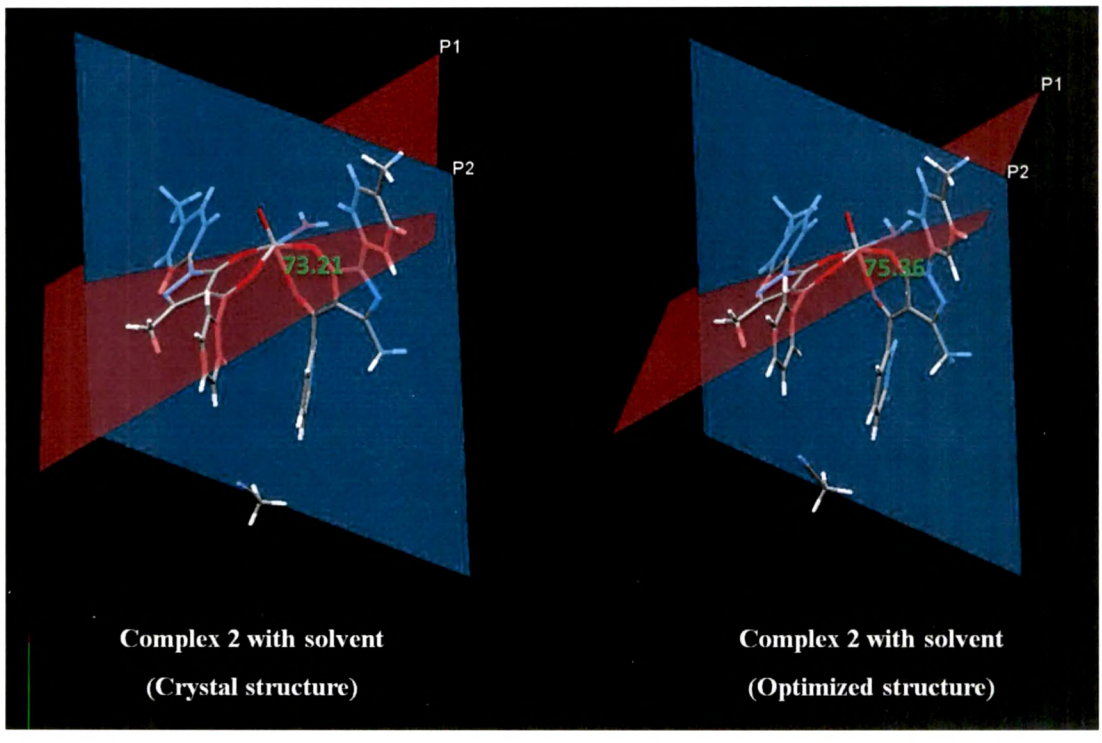

Figure 4.5. Dihedral angle between the plane P_1 (C23O1V1O2C33C24) and P_2 (C3O3V1O13C13C4) of the (*a*) crystal structure and (*b*) optimized structure in complex **2** (with solvent).

The angle between the coordinated water molecule and oxo group (O5-V1-O6) increased by 80.48°. The angles O1-V1-O4, O2-V1-O4, O2-V1-O3, O4-V1-O6, O1-V1-O5 and O3-V1-O5 show an increase by 81.27°, 46.01°, 83.82°, 33.08°, 15.92° and 22.94°, respectively, while the angles O2-V1-O6 and O1-V1-O3 show decrease by 44.64° and 38.73°, respectively. The comparison of the angles of the structure without solvent results in deviation from the experimental results. The total energies of the complex **2** with solvent and complex **2** without solvent are also calculated. The calculated total energy for complex **2** with solvent is obtained –10.793 keV in contrast

to the -10.158 keV in the case of complex **2** without solvent. The total energy of complex **2** with solvent is less than the complex **2** without solvent. Thus, the twisted geometry of the complex **2** with solvent is more stable than the geometry of complex **2** without solvent.

4.3.2 HOMO and LUMO analysis

The analysis of the wave function indicates that the electron adsorption corresponds to the transition from the ground state to the first excited state and is mainly described by one-electron excitation from the highest occupied molecular orbital to the lowest unoccupied molecular orbital. The HOMO and LUMO orbitals for the *syn* and *anti* conformations of complex **1** are shown in Figure 4.6.

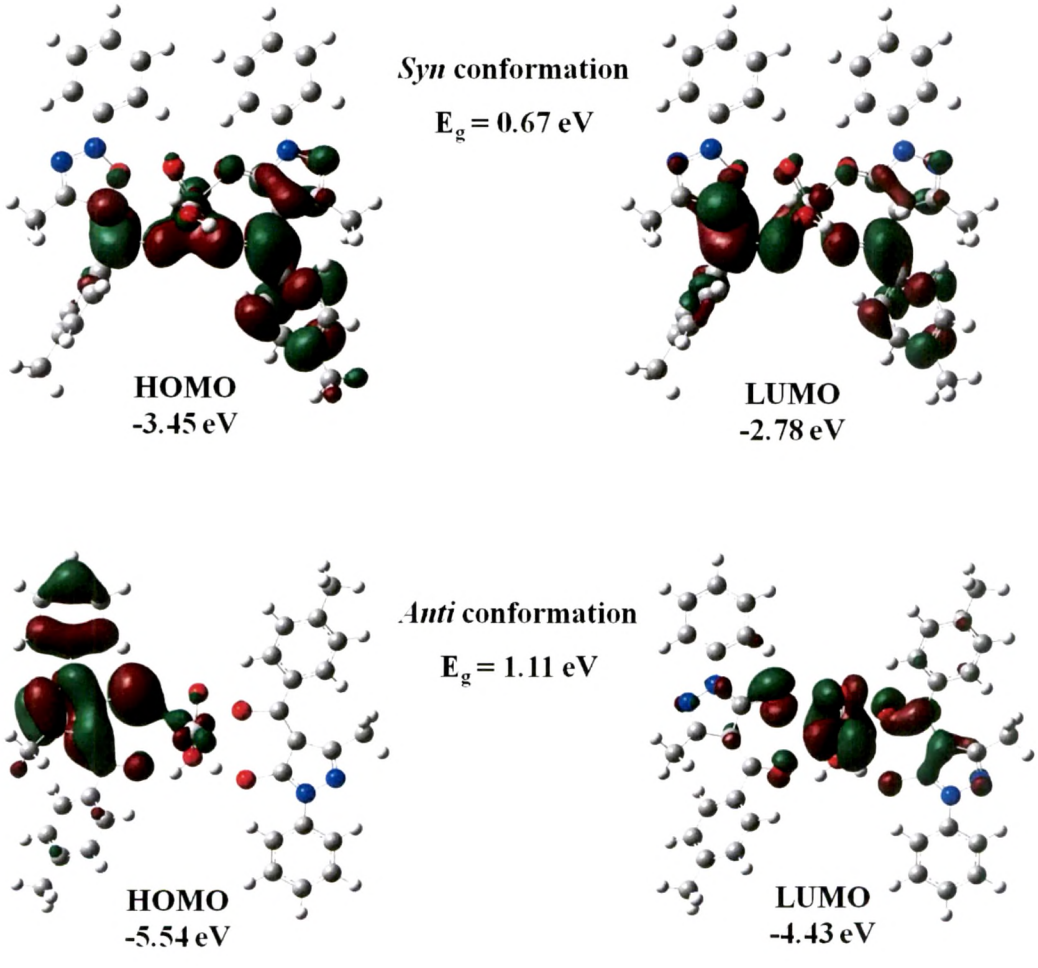

Figure 4.6. HOMO and LUMO compositions of the Frontier molecular orbitals of complex **1**.

The energy gap reflects the chemical activity of a molecule. As seen in Figure 4.6, in *syn* conformation HOMO is localized on the toluoyl and pyrazolone ring of the ligand, while in *anti* conformation HOMO is localized on the phenyl and pyrazolone ring. In the *syn* conformation LUMO is localized on the toluoyl rings of both the ligands, while in *anti* conformation LUMO is localized on the metal centre and donor oxygen atoms. The energy of HOMO is often associated with the electron-donating ability of a molecule; such that high energy values of HOMO are likely to indicate a tendency of the molecule to donate electrons. The energy of LUMO is related to the electron affinity. The binding ability of the ligand to the metal increases with increasing HOMO energy values. The HOMO and LUMO orbitals for the complex **2** with solvent and without solvent are shown in Figure 4.7.

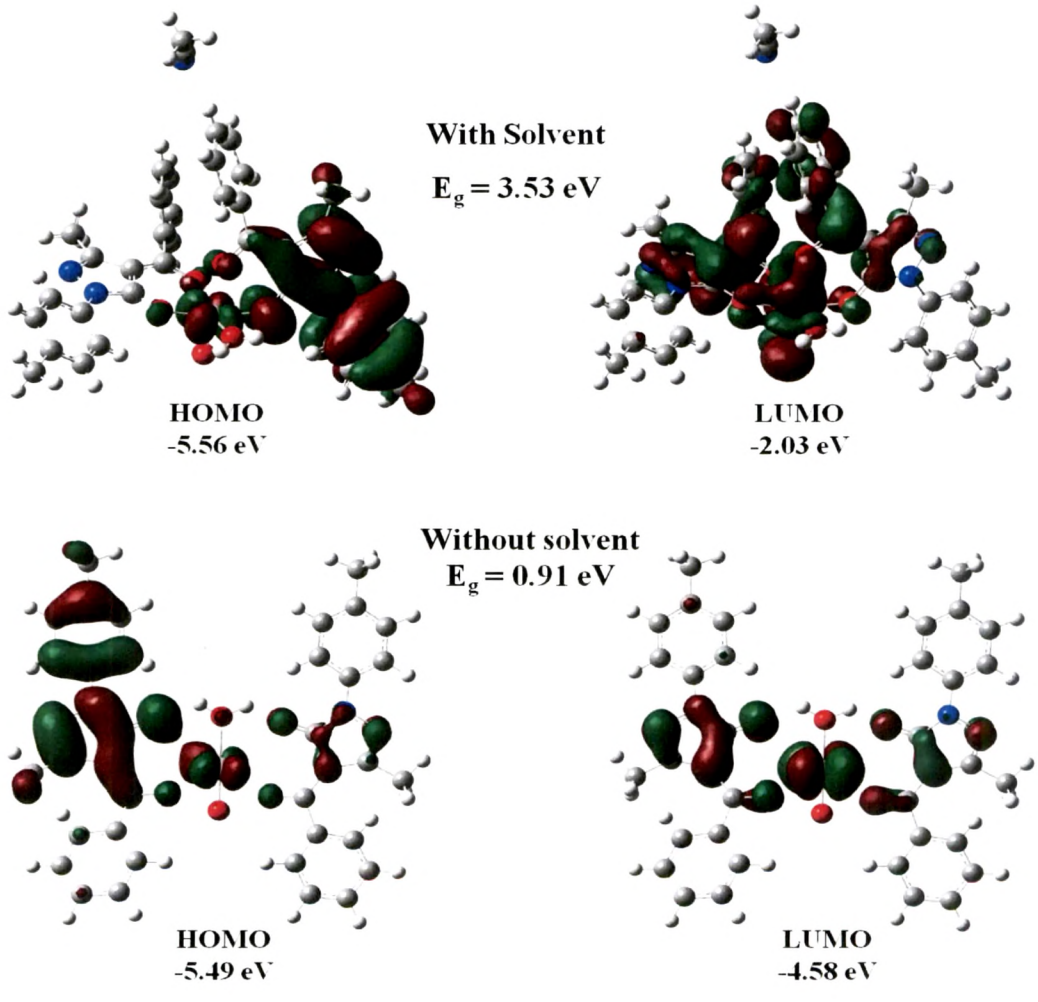

Figure 4.7. HOMO and LUMO compositions of the frontier molecular orbitals of complex **2**.

4.3.3 Electronic density of states analysis

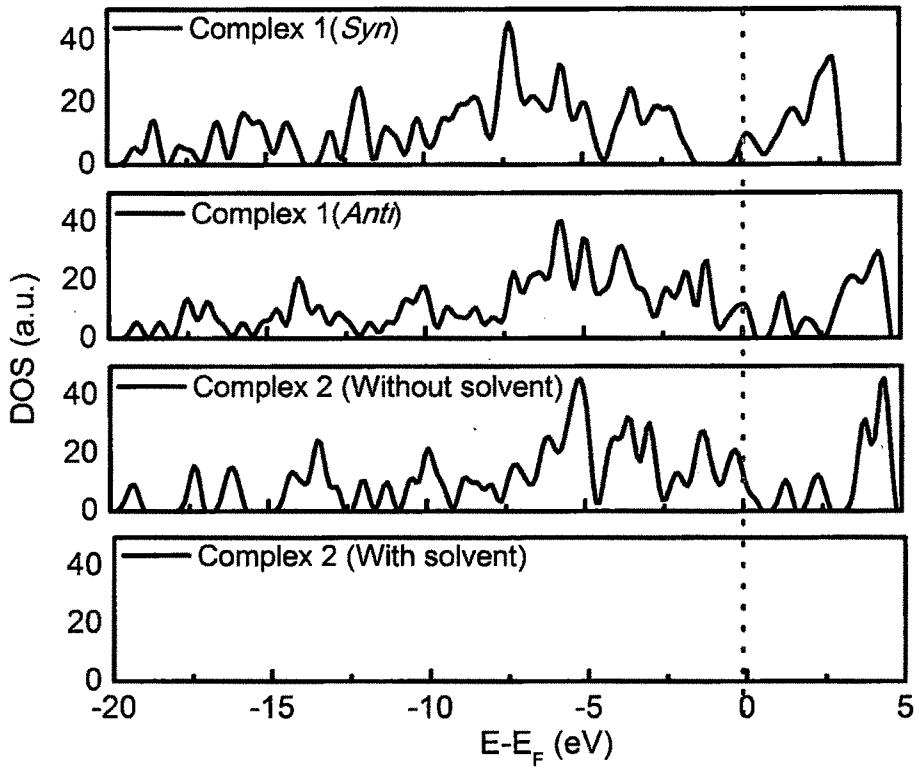

Figure 4.8. Electronic density of states of *syn* configuration, *anti*, twisted without solvent and twisted with solvent configuration complexes respectively, the Fermi level is set to be 0 eV.

The electronic densities of states (DOS) of *syn*, *anti*, twist conformation without solvent and twisted with solvent conformation complexes are shown in Figure 8. The most significant difference is observed at Fermi level where the density as well as shape of the spectral changes going from *syn* to twisted complexes. An apparent gap just above the Fermi level in the case of ligand vanishes which indicates a metallic behavior of complexes. A sharp high peak with two shoulders turns to the less intense peak shifted to the lower energy side. Another interesting observation is the opening of the gap (about 1.74 eV) close to Fermi level in between -2.0 and 1 eV is wider in the case of *syn* and twist-solvent complexes. The appearance of complex induced hybrid states near to Fermi energy in present study (*see* Figure 4.8) explains the spectral shift observed during experiments. Furthermore, the main contribution to HOMO is localized on the toluoyl and pyrazolone ring of the ligand while the *d*-orbitals of the metal ion contribute to the LUMO consistent with Figure 4.6. The shift

in HOMO and LUMO energy difference from complexes may be due to the Columbic and coordination effects and van der Waals interactions. The Columbic effects are produced by the charge distribution which might alter the energy level of metal complexes [28].

In density of states, the complexes producing the bonding and *anti*-bonding like hybrid orbitals below and above the middle of metal *d*-band. It is clear that the electronic structure and the gap width are very sensitive to the changes in complexes. Indeed, there is a change in the density of states in between -20 to -15 eV and -10 to -5 eV. The most of the states look similar in the range of -10 to -5 eV, shows that all complexes derived from one *syn* complex.

4.4 Conclusions

In this work, we have studied the geometry of some oxovanadium(IV) complexes of 4-acyl pyrazolone ligands using a theoretical approach to figure out the electronic structures of these category of complexes. The DFT calculations at GGA potentials of PBE have been carried out to identify the most stable geometry of complex **1** between *syn* and *anti* conformation and complex **2** between twisted (with solvent) and *syn* (without solvent). The bond lengths and bond angles of optimized structures were compared with the experimental results obtained from the crystal structure of the complexes using XRD. Comparison of the calculated bond lengths and bond angles revealed that there is a reasonably good agreement for some of them but some deviations are also noted. The noted discrepancy can be attributed to the fact that the calculations have been performed on a single molecule in the gaseous state contrary to the experimental values recorded in the presence of intermolecular interactions as well as to the different methods used for the calculation of HOMO/LUMO and electronic states. The total energy of all the optimized structures has been calculated to obtain the most stable conformation. The energy of HOMO and LUMO frontier molecular orbital has also been calculated. According to the results the most stable geometry of the complex **1**, in agreement with the X-ray single crystal data, is *syn* conformation. The most stable geometry of the complex **2**, in agreement with the X-ray single crystal data, is twisted (with solvent) geometry.

4.5 References

[1] (*a*) C. J. Cramer, *Essentials of Computational Chemistry* (2nd ed.), Wiley, **2004**; (*b*) T. Schlick, *Molecular Modeling and Simulation*, Springer, **2002**.

[2] (*a*) K. I. Ramachandran, G. Deepa, K. Namboori, *Computational Chemistry and Molecular Modeling*, Springer, **2008**; (*b*) E. Lewars, *Computational Chemistry: Introduction to the Theory and Applications of Molecular and Quantum Mechanics*, Kluwer Academic Publishers, New York, USA, **2004**.

[3] (*a*) P. Deglmann, F. Furche, R. Ahlrichs, *Chem. Phys. Lett.*, **2002**, *362*, 511-518; (*b*) M. Sierka, A. Hogekamp, R. Ahlrichs, *J. Chem. Phys.*, **2003**, *118*, 9136-9148.

[4] S. Das, S. Karmakar, D. Saha, S. Baitalik, *Inorg. Chem.*, **2013**, *52*, 6860-6879 and references cited therein.

[5] F. D. Proft, P. Geerlings, *Chem. Rev.*, **2001**, *101*, 1451–1464.

[6] (*a*) H. Tanak, *J. Phys. Chem. A*, **2011**, *115*, 13865–13876; (*b*) H. Tanak, *Int. J. Quantum Chem.*, **2012**, *112*, 2392–2402.

[7] M. M. Kimani, C. A. Bayse, J. L. Brumaghim, *Dalton Trans.*, **2011**, *40*, 3711–3723.

[8] S. Das, D. Saha, S. Mardanya, S. Baitalik, *Dalton Trans.*, **2012**, *41*, 12296–12310.

[9] T. Samanta, B. K. Rana, G. Roymahapatra, S. Giri, P. Mitra, R. Pallepogu, P. K. Chattaraj, J. Dinda, *Inorg. Chim. Acta*, **2011**, *375*, 271-279.

[10] S. Mistri, E. Zangrando, S. C. Manna, *Inorg. Chim. Acta*, **2013**, *405*, 331-338.

[11] (*a*) B. Machura, M. Wolff, D. Tabaka, Y. Ikeda, K. Hasegawa, *Polyhedron*, **2012**, *39*, 76-84; (*b*) B. Machura, M. Wolff, I. Gryca, R. Kruszynski, *Polyhedron*, **2012**, *40*, 93-104; (*c*) B. Machura, M. Wolff, E. Benoist, Y. Coulais, *J. Organomet. Chem.*, **2013**, *724*, 82-87; (*d*) B. Machura, M. Wolff, W. Cieślik, R. Musiol, *Polyhedron*, **2013**, *51*, 263-274.

[12] (*a*) A. Butler, M. J. Clague, G. E. Meister, *Chem. Rev.*, **1994**, *94*, 625-638; (*b*) H. Sigel, A. Sigel, (eds.) *Metal Ions in Biological Systems*, New York, **1995**, vol. 31; (*c*) A. S. Tracey, D. C. Crans, (eds.) *Vanadium Compounds, ACS Symposium Series* 711, , ACS, Washington DC, **1998**; (d) K. H.

Thompson, C. Orvig, *Coord. Chem. Rev.*, **2001**, *219*, 1033-1053; (*e*) R. R. Eady, *Coord. Chem. Rev.*, **2003**, *237*, 23-30.

[13] (*a*) T. Hirao, *Chem. Rev.*, **1997**, *97*, 2707-2724; (*b*) H.-L. Wu, B.-J. Uang, *Tetrahedron: Asymmetry*, **2002**, *13*, 2625–2628; (*c*) C. Bolm, *Coord. Chem. Rev.* **2003**, *237*, 245-256; (*d*) A.G. J. Ligtenbarg, R. Hage, B.L. Feringa, *Coord. Chem. Rev.* **2003**, *237*, 89-101; (*e*) M. Bühl, R. Schurhammer, P. Imho, *J. Am. Chem. Soc*, **2004**, *126*, 3310-3320; (*f*) G. Santoni, G. Licini, D. Rehder, *Chem.-Eur. J.* **2003**, *9*, 4700-4708; (*i*) C. Drago, L. Caggiano, R. F. W. Jackson, *Angew. Chem., Int. Ed.*, **2005**, *44*, 7221-7223 (*j*) F. Cavani, N. Ballarini, A. Cericola, *Catal. Today* **2007**, *127,* 113-131; (*k*) S. Takizawa, T. Katayama, H. Sasai, *Chem. Commun.* **2008**, 4113-4122.

[14] (*a*) K. Kustin,; J. C. Pessoa, D. C. Crans, (Eds.), *Vanadium: The Versatile Metal, American Chemical Society*, Washinton, DC, **2007**; (*b*) D. Rehder, *Bioinorganic Vanadium Chemistry*, John Wiley & Sons: Chichester, U.K., **2008**; (*c*) S. Takizawa, T. Katayama, H. Sasai, *Chem. Commun.*, **2008**, 4113-4122; (*d*) S. L. Jain, B. S. Rana, B. Singh, A. K. Sinha, A. Bhaumik, M. Nandi, B. Sain, *Green Chem.*, **2010**, *12*, 374–377; (*e*) S. K. Hanson, R. Wu, L. A. P. Silks, *Org. Lett.*, **2011**, *13*, 1908-1911; (*f*) N. Mizuno, K. Kamata, *Coord. Chem. Rev.*, **2011**, *255,* 2358– 2370; (*g*) M. Kirihara, *Coord. Chem. Rev.*, **2011**, *255*, 2281-2302; (*h*) J. A. L. da Silva, J. J. R. F. da Silva, A. J. L. Pomberio, *Coord. Chem. Rev.*, **2011**, *255*, 2232-2248; (*i*) J. -Q. Wu, Y. -S. Li, *Coord. Chem. Rev.*, **2011**, *255*, 2303-2314; (*j*) M. R. Maurya, A. Kumar, J. C. Pessoa, *Coord. Chem. Rev.*, **2011**, *255*, 2315-2344; (*k*)R. Kwahara, K.-i Fujita, R. Yamaguchi, *J. Am. Chem. Soc.*, **2012**, *134*, 3643-3646.

[15] I. Correia, J. C. Pessoa, M. T. Duarte, R. T. Henriques, M. F. M. Piedade, L. F. Veiros, T. Jakusch, T. Kiss, A. Dörnyei, M. M. C. A. Castro, C. F. G. C. Geraldes, F. Avecilla, *Chem. Eur. J.*, **2004**, *10*, 2301-2317.

[16] (*a*) J. C. Pessoa, M. J. Carholda, I. Cavaco, I. Correia, M. T. Duarte, V. Felix, R. T. Henriques, M. F. M. Piedade, I. Tomaz, *J. Chem. Soc., Dalton Trans.*, **2002**, 4407–4415; (*b*) D. del Rio, A. Galindo, R. Vicente, C. Mealli, A. Inco, D. Masi, *Dalton Trans.*, **2003**, 1813–1820; (*c*) C. Wikete, P. Wu, G. Zampella, L. D. Gioia, D. Rehder, *Inorg. Chem.*, **2007**, *46*, 196-207; (*d*) J. Charppová, P. Schwendt, M. Sivák, M. Repiský, V. G. Malkin, J. Marek, Dalton Trans., 2009, 465-473; (*e*) C. E. Johnson, E. A. Kysor, M. Findlater,

J. P. Jesinski, A. S. Metell, J. W. Queen, C. D. Abernethy, *Dalton Trans.*, **2010**, *39*, 3482-3488; (*f*) L. Álvarez, A. Grirrane, R. Moyano, E. Álvarez, A. Pastor, A. Galindo, *Polyhedron*, **2010**, *29*, 3028-3035; (g) H. H. Monfared, S. Alavi, R. Bikas, M. Vahedpour, P. Mayer, *Polyhedron*, **2010**, *29*, 3355-3362; (*h*) S. Spraoules, T. Weyhermüller, S. DeBeer, K. Wieghardt, *Inorg. Chem.*, **2010**, *49*, 5241-5261; (*i*) C. Cordelle, D. Agustin, J. -C. Daran, R. Poli, *Inorg. Chimi. Acta*, **2010**, *364*, 144-149; (*j*) A. Mota, J. P. Hallett, M. L. Kuznetsov, I. Correia, *Phys. Chem. Chem. Phys.*, **2011**, *13*, 15094-15102; (*k*) G. Micera, E. Garribba, *Int. J. Quant. Chem.*, **2012**, *112*, 2486-2498; (*l*) A. Jana, S. Konar, T. N. Mandal, K. Das, S. Ray, A. Sarkar, C. -M. Liu, S. K. Kar, *Polyhedron*, **2012**, *46*, 105-112; (*m*) P. Mondal, A. Hens, K. K. Rajak, *Polyhedron*, **2013**, *54*, 228-236; (*n*) V. Jodaian, M. Mirzaei, M. Arca, M. C. Aragoni, V. Lippolis, E. Tavakoli, N. S. Langeroodi, *Inorg. Chimi. Acta*, **2013**, *400*, 107-114; (*o*) S. Chaudhuri, S. Bera, M. K. Biswas, A. S. Roy, T. Weyhermüller, P. Ghosh, *Inorg. Chem. Front.*, **2014**, *1*, 331-341; (*p*) H. Hosseini-Monfared, R. Bikas, P. Mahboubi-Anarjan, A. J. Blake, V. Lippolis, N. B. Arslan, C. Kazak, *Polyhedron*, **2014**, *69*, 90–102.

[17] (*a*) F. Marchetti , C. Pettinari, R. Pettinari, *Coord. Chem. Rev.*, **2005**, *249*, 2909-2945; (*b*) G. Xu, L. Liu, L. Zhang, G. Liu, D. Jia, J. Lang, *Struct. Chem.*, **2005**, *16*, 431-437; (*c*) Z. Hayvali, *Transit. Met. Chem.*, **2009**, *34*, 97-101; (*d*) P. M. V. Kumar, P. K. Radhakrishnan, *Polyhedron*, **2010**, *29*, 2335-2344;

[18] (*a*) F. Bao, X Lü, Y. Qiao, G. Gui, H. Gao, Q. Wu, *Appl. Organometal. Chem.*, **2005**, *19*, 957–963; (*b*) F. Bao, R. Ma, X. Lü, G. Gui, Q. Wu, *Appl. Organometal. Chem.*, **2006**, *20*, 32-38.

[19] F. Marchetti, C. Pettinari, C. D. Nicola, R. Pettinari, A. Crispini, M. Crucianelli, A. D. Giuseppe, *Appl. Catal. A: Gen.*, **2010**, *378*, 211-233.

[20] S. Parihar, S. Pathan, R. N. Jadeja, A. Patel, V. K. Gupta, *Inorg. Chem.*, **2012**, *51*, 1152-1161.

[21] S. Parihar, R. N. Jadeja, V. K. Gupta, *RSC Adv.*, **2014**, *4*,10295–10302.

[22] (*a*) R. N. Jadeja, K. M. Vyas, V. K. Gupta, R. G. Joshi, C. R. Prabha, *Polyhedron*, **2012**, *31*, 767-778; (*b*) K. M. Vyas, R. G. Joshi, R. N. Jadeja, C. R. Prabha, V. K. Gupta, *Spectrochim. Acta A*, **2011**, *84*, 256-268; (*c*) R. N. Jadeja, S. Parihar, K. Vyas, V. K. Gupta, *J. Mol. Struct.*, **2012**, *1013*, 86-94;

(*d*) R. N. Jadeja, M. Chhatrola, V. K. Gupta, *Polyhedron*, **2013**, *63*, 117-126; (*e*) K. M. Vyas, R. N. Jadeja, D. Patel, R. V. Devkar, V. K. Gupta, *Polyhedron*, **2013**, *65*, 262-274.

[23] (*a*) E. R. Menzel, D. R. Lorenz, J. R. Wasson, K. R. Radigan, B. J. McCormik, *J. Inorg. Nucl. Chem.*, **1976**, *3*, 993-996; (*b*) B.A. Uzoukwu, *Synth. React. Inorg. Met. Org. Chem.*, **1992**, *22*, 185-194; (*c*) R. C. Maurya, S. Rajput, *Synth. React. Inorg. Met. Org. Chem.*, **2003**, *33*, 1877-1894; (*d*) R. C. Maurya, H. Singh, *Synth. React. Inorg. Met. Org. Chem.*, **2004**, *34*, 269-290.

[24] <http://www.pwscf.org>.

[25] H. J. Monkhorst, J. D. Pack, *Phys. Rev. B*, **1976**, *13*, 5188–5192.

[26] M. J. Frisch et al., Gaussian 03, in: Revision B.03, Gaussian Inc., Pittsburgh, PA, **2003**.

[27] C. Lee, W. Yang, R. G. Parr, *Phys. Rev. B*, **1988**, *37*, 785–789.

[28] C. K. Modi, P. M. Trivedi, S. K. Gupta, P. K. Jha, *J. Incl. Phenom. Macrocycl. Chem.*, **2012**, *74*, 117-127.

Spectrochimica Acta Part A: Molecular and Biomolecular Spectroscopy 128 (2014) 447–451

Contents lists available at ScienceDirect

Spectrochimica Acta Part A: Molecular and Biomolecular Spectroscopy

journal homepage: www.elsevier.com/locate/saa

A comparative study of experimental and theoretical results of conformations of oxovanadium(IV) complexes with 4-acyl pyrazolone ligands using DFT method

Sanjay Parihar [a], Sanjeev K. Gupta [b], R.N. Jadeja [a,*], Prafulla K. Jha [c,*]

[a] Department of Chemistry, Faculty of Science, The M. S. University of Baroda, Vadodara 390002, Gujarat, India
[b] Department of Physics, Michigan Technological University, Houghton, MI 49931, USA
[c] Department of Physics, Faculty of Science, The M. S. University of Baroda, Vadodara 390002, Gujarat, India

HIGHLIGHTS

- Comparison of crystal structures and optimized structures of complexes.
- Calculation and comparison of total energy of *syn*, *anti* and *twisted* geometries.
- Quantum chemical parameters (HOMO–LUMO) and energy gap were calculated.
- Most stable geometry of complexes was found theoretically.

GRAPHICAL ABSTRACT

Oxovanadium(IV) complex of 4-acylpyrazolone showing *twisted* geometry

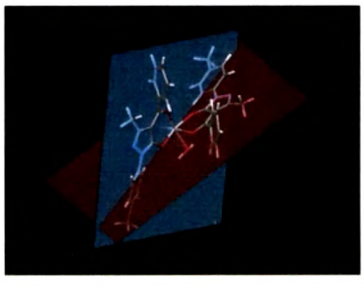

ARTICLE INFO

Article history:
Received 15 October 2013
Received in revised form 19 February 2014
Accepted 21 February 2014
Available online 12 March 2014

Keywords:
Acylpyrazolone
DFT
HOMO
Oxovanadium(IV)
Geometry optimization

ABSTRACT

The optimized structures and electronic properties of the oxovanadium(IV) complexes containing 4-acyl pyrazolone ligands were calculated using density functional theory. The total energies of both the complexes were calculated e.g. *syn* and *anti* conformation of complex 1 and complex 2 with and without solvent. The calculated total energy for *syn* conformation was −10.162 keV, while total energy for *anti* conformation was −10.155 keV. Similarly, the calculated total energy for complex 2 with solvent was obtained −10.793 keV, while total energy for complex 2 without solvent was −10.158 keV. The total energy calculation shows that *syn* conformation is more stable in complex 1, while complex 2 is more stable in twisted geometry with solvent. In order to investigate the electronic properties of ligands and complexes, quantum chemical parameters, such as the highest occupied molecular orbital energy (HOMO), the lowest unoccupied molecular orbital energy (LUMO), and energy gap were calculated. The theoretically calculated data of the complexes are in good agreement with the data obtained by the single-crystal X-ray diffraction analysis.

Introduction

The coordination chemistry and reactivity of transition metal complexes containing 4-acyl pyrazolone ligands have attracted

* Corresponding authors. Tel.: +91 265 2795552 (R.N. Jadeja), Tel.: +91 278 2422650 (P.K. Jha).
E-mail addresses: rajendra_jadeja@yahoo.com (R.N. Jadeja), prafullaj@yahoo.com (P.K. Jha).

http://dx.doi.org/10.1016/j.saa.2014.02.138
1386-1425/

List of publications

International Journals

[1] **Sanjay Parihar**, Soyeb Pathan, R. N. Jadeja, Anjali Patel, Vivek K. Gupta, "*Synthesis and Crystal Structure of an Oxovanadium(IV) Complex with a Pyrazolone Ligand and Its Use as a Heterogeneous Catalyst for the Oxidation of Styrene under Mild Conditions*", ***Inorg. Chem.***, **2012**, *51*, 1152-1161.

[2] R. N. Jadeja, **Sanjay Parihar**, Komal Vyas, Vivek K. Gupta, "*Synthesis and crystal structure of a series of pyrazolone based Schiff base ligands and DNA binding studies of their copper complexes*", ***J. Mol. Struct.***, **2012**, *1013*, 86-94.

[3] **Sanjay Parihar**, R. N. Jadeja, Vivek K. Gupta, "*Novel oxovanadium(IV) complexes with 4-acyl pyrazolone ligands: synthesis, crystal structure and catalytic activity towards the oxidation of benzylic alcohols*", ***RSC Adv.***, **2014**, *4*, 10295-10302.

[4] **Sanjay Parihar**, Sanjeev K. Gupta, R. N. Jadeja, Prafulla K. Jha, "*A comparative study of experimental and theoretical results of conformations of oxovanadium(IV) complexes with 4-acyl pyrazolone ligands using DFT method*", ***Spectrochim. Acta: A***, **2014**, *128*, 447-451.

[5] **Sanjay Parihar**, Vinod P. Boricha, R. N. Jadeja, "*Pyrazolone as a recognition site: Rhodamine 6G-based fluorescent probe for selective recognition of* Fe^{3+} *in acetonitrile-aqueous solution*", ***Luminescence***, **2014**, DOI: 10.1002/bio.2709.

[6] **Sanjay Parihar**, R. N. Jadeja, Vivek K. Gupta, "C_3 *Symmetric vanadium(III) complexes with O,N-chelating hexadentate tripodal ligands of pyrazolone*", ***RSC Adv.***, **2014**, *4*, 43994-43997.

[7] Naresh Sharma, **Sanjay Parihar**, R. N. Jadeja, Rajni Kant, Vivek K. Gupta, "*Crystal structure of (Z)-1-(3,4-dichlorophenyl)-3-methyl-4-[(naphthalen-1-ylamino)(p-tolyl)methylidene]-1H-pyrazol5(4H)-one*", ***Acta Cryst.***, **2014**, *E70*, o955–o956.

[8] Naresh Sharma, **Sanjay Parihar**, R. N. Jadeja, Rajni Kant, Vivek K. Gupta, "*Crystal structure of (4Z)-1-(3,4-dichlorophenyl)-4-[hydroxy(4-*

methylphenyl)methylidene]-3-methyl-4,5-dihydro-1Hpyrazol-5-one", ***Acta Cryst.*, 2014**, *E70*, o1136–o1137.

[9] **Sanjay Parihar**, R. N. Jadeja, Vivek K. Gupta, "*Crystal structure study and catalytic application of Cu(II) complexes derived from acylpyrazolone Schiff bases*", ***Cryst. Res. Technol.*, 2014** (*Communicated*).

Book Chapters

[1] **Sanjay Parihar**, R. N. Jadeja, "*Catalysis using Oxovanadium(IV) complexes of 4-Acylpyrazolone Ligand*" in ***Advances in Chemistry Research*** (Ed: J. C. Taylor), **2014**, *Vol. 22, Ch. 9*, 217-229.

National/ International Conferences

[1] Poster presented in the '***National conference on challenges to chemical sciences in twenty first century***' held on **1-2 February 2011** at Department of Chemistry, Hemchandracharya North Gujarat University, Patan.

[2] Oral presentation in the '***International conference on Green chemistry***' held on **7-9 December 2011** at Central University of Rajasthan, Jaipur.

[3] Poster Presented in the '***National conference on chemical sciences in new millennium***' held on **8th January 2012** at Pacific University, Udaipur.

[4] Poster presented in the one day seminar on '***Preparation and characterization of crystalline and non-crystalline solids (PCCNS)***' held on **2nd November 2012** at Department of Physics, The M. S. University of Baroda, Vadodara.

[5] Poster presented in the '***Modern Trends in Inorganic Chemistry (MTIC-XV)***' held on **13-16 December 2013** at Indian Institute of Technology, Roorkee, Uttarakhand.